

Temperature-dependent phonon shifts in monolayer MoS₂

Nicholas A. Lanzillo, A. Glen Birdwell, Matin Amani, Frank J. Crowne, Pankaj B. Shah, Sina Najmaei, Zheng Liu, Pulickel M. Ajayan, Jun Lou, Madan Dubey, Saroj K. Nayak, and Terrance P. O'Regan

Citation: *Applied Physics Letters* **103**, 093102 (2013); doi: 10.1063/1.4819337

View online: <http://dx.doi.org/10.1063/1.4819337>

View Table of Contents: <http://scitation.aip.org/content/aip/journal/apl/103/9?ver=pdfcov>

Published by the [AIP Publishing](#)



Goodfellow

metals • ceramics • polymers
composites • compounds • glasses

Save 5% • Buy online
70,000 products • Fast shipping

www.goodfellowusa.com

Temperature-dependent phonon shifts in monolayer MoS₂

Nicholas A. Lanzillo,¹ A. Glen Birdwell,² Matin Amani,² Frank J. Crowne,² Pankaj B. Shah,² Sina Najmaei,³ Zheng Liu,³ Pulickel M. Ajayan,³ Jun Lou,³ Madan Dubey,² Saroj K. Nayak,^{1,4} and Terrance P. O'Regan²

¹*Department of Physics, Applied Physics, and Astronomy, Rensselaer Polytechnic Institute, 110 8th Street, Troy, New York 12180, USA*

²*Sensors and Electron Devices Directorate, US Army Research Laboratory, Adelphi, Maryland 20783, USA*

³*Department of Mechanical Engineering and Materials Science, Rice University, Houston, Texas 77005, USA*

⁴*School of Basic Sciences, Indian Institute of Technology, Bhubaneswar, India 751007*

(Received 9 July 2013; accepted 12 August 2013; published online 26 August 2013)

We present a combined experimental and computational study of two-dimensional molybdenum disulfide and the effect of temperature on the frequency shifts of the Raman-active E_{2g} and A_{1g} modes in the monolayer. While both peaks show an expected red-shift with increasing temperature, the frequency shift is larger for the A_{1g} mode than for the E_{2g} mode. This is in contrast to previously reported bulk behavior, in which the E_{2g} mode shows a larger frequency shift with temperature. The temperature dependence of these phonon shifts is attributed to the anharmonic contributions to the ionic interaction potential in the two-dimensional system. © 2013 AIP Publishing LLC.
[\[http://dx.doi.org/10.1063/1.4819337\]](http://dx.doi.org/10.1063/1.4819337)

Molybdenum disulfide (MoS₂) is a transition-metal dichalcogenide consisting of covalently bound S-Mo-S layers held together by the weak van der Waals interaction and is of great research interest due to its potential uses in electronic and optical devices. MoS₂ shows a number of interesting features when confined to a single monolayer—most notably an indirect-to-direct electronic band gap transition^{1–3}—accompanied by an large increase in the photoluminescence (PL) quantum yield.⁴ The room-temperature mobility of MoS₂ is comparable to that of graphene nanoribbons, and has been predicted theoretically to be as high as 400 cm² V⁻¹ s⁻¹ when optical phonon scattering and intra/intervalley deformation potential couplings are included,⁵ although fabricated transistors have shown a more modest mobility of around half this value.⁶

The vibrational properties of bulk, few layer, and monolayer MoS₂ have been studied both experimentally^{7–12} and theoretically.^{13–15} One of the most pronounced effects of confining the system to a strictly 2-dimensional geometry in the monolayer is the redshift of the Raman-active A_{1g} mode and blueshift of the Raman-active E_{2g} phonon mode with decreasing number of layers.¹⁴ The unexpected blueshift of the E_{2g} peak was shown to be due to dielectric screening of the long-range Coulomb interaction,¹³ while the redshift of the A_{1g} mode is in line with the classical picture of a harmonic potential. Work involving the effect of strain shows that the in-plane E_{2g} mode is sensitive to strain, while the out-of-plane A_{1g} mode shows a weak strain dependence.⁹ These two Raman-active mode also show distinct doping dependence; with the A_{1g} mode decreasing in frequency with increased electron concentration and the E_{2g} mode showing an overall weak dependence on electron concentration.⁷ This difference is attributed to the stronger coupling to electrons of the A_{1g} mode compared with the E_{2g} mode.

While the temperature dependence of the Raman active peaks has been investigated for the bulk crystal,⁸ the temperature effect on the monolayer has not been studied. In the

bulk crystal, both the A_{1g} and E_{2g} peaks shift toward lower frequencies with increasing temperature, and the temperature coefficient of the E_{2g} mode is larger in magnitude than that of the A_{1g} mode. Here, we show using Raman spectroscopy along with finite-temperature molecular dynamics simulations that for the monolayer, both peaks show a redshift with increasing temperature but the magnitude of the frequency shift is larger for the A_{1g} mode than for the E_{2g} mode. Our molecular dynamics simulations were performed with the Car-Parrinello Molecular Dynamics (CPMD) code¹⁶ using Hartwigsen-Goedecker-Hutter (HGH) gradient-corrected pseudopotentials¹⁷ and a plane wave cutoff energy of 80 Rydberg. Our supercell contained 48 atoms and k-point sampling was restricted to the Γ -point of the Brillouin Zone. We have included 14 Å of vacuum separating periodic images of the monolayer. The geometry was relaxed until the forces on the atoms were less than 10⁻² eV/Å, and we have found the average Mo-S bond length to be 2.41 Å, which is within 0.05 Å of the optimized structures found in the previous work.^{13,14} In order to investigate the effect of temperature on the phonon spectra, we have performed Car-Parrinello¹⁸ CPMD simulations for the system in the crystal phase. The system was kept close to the Born-Oppenheimer surface through repeated quenching. The simulations were allowed to evolve for 100 ps using a timestep of 4 a.u. and a fictitious electron mass of 400 a.u. The phonon spectrum was derived from the Fourier transform of the velocity auto-correlation function. The resolution in frequency space is on the order of 2 cm⁻¹. These calculations were run on 1024 processors of the IBM BG/L supercomputer.

Single layer MoS₂ films were grown directly on 285 nm SiO₂/Si substrate by chemical vapor deposition (CVD) using the procedure described in detail by Najmaei *et al.*^{19,20} Hydrothermally grown MoO₃ nanoribbons were dispersed onto auxiliary silicon substrates and placed inside a tube furnace surrounded by the growth substrate. Sulfur powder was sublimated upstream near the opening of the furnace at an

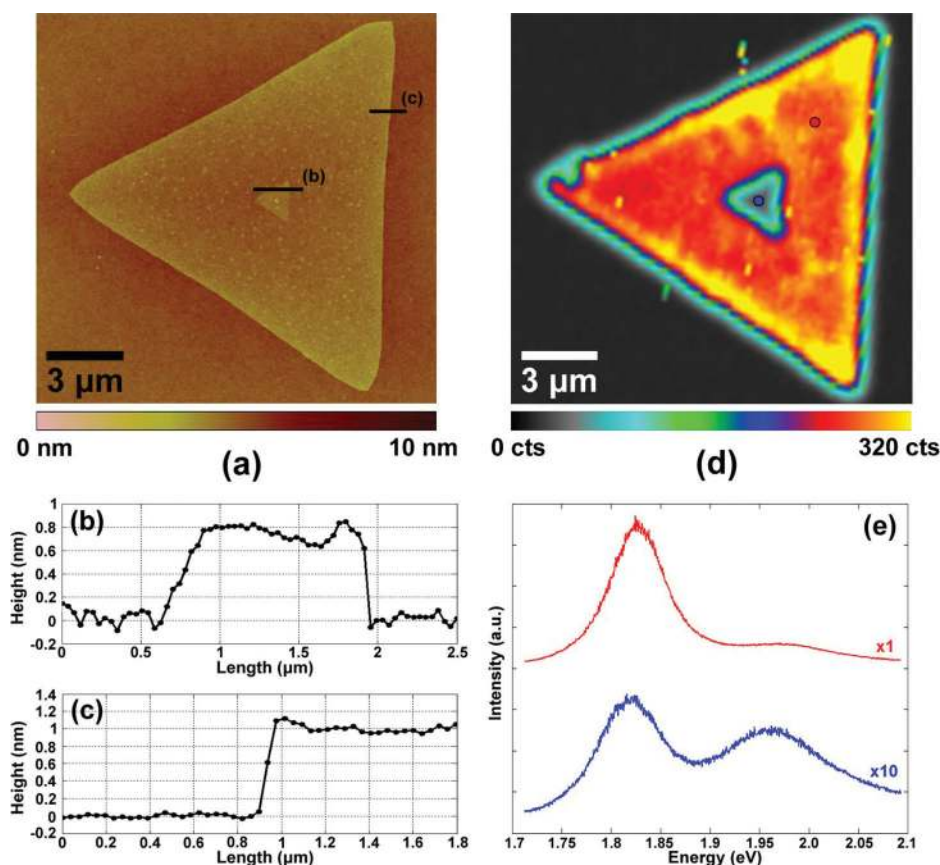


FIG. 1. AFM image of a typical MoS₂ crystal (a), step height measurement of the monolayer to bilayer step (0.7 nm) (b), step height measurement from substrate to monolayer (0.9 nm) (c), PL intensity map of the same MoS₂ crystal (d), and individual spectra for the monolayer (red) and bilayer (blue) regions (e).

approximate temperature of 600 °C while the furnace was heated to a peak temperature of 850 °C under a constant flow of nitrogen and was held at this set point for 10 to 15 min and then cooled to room temperature. This resulted in incomplete growth of triangular MoS₂ domains which were primarily monolayer but occasionally contained a small bilayer region in the center.

Micro-Raman and PL measurements were performed with a WITec Alpha 300RA system using the 532 nm line of a frequency-doubled Nd:YAG laser as the excitation source. The spectra were measured in the backscattering configuration using a 100× objective and either a 600 or 1800 grooves/mm grating. The spot size of the laser was ~342 nm resulting in an incident laser power density of ~140 μW/μm². This laser power was found to be sufficiently low not to cause any shifting in the both the in-plane and out-of-plane modes of the Raman signature.²¹ Single point Raman measurements were performed on the same location in the sample over the temperature range from 30 to 175 °C using a heating stage. The location was determined via Raman mapping the selected crystal at each temperature set, after allowing at least 30 min for thermal stabilization of the sample and optics. In addition, atomic force microscopy (AFM) was utilized to confirm the thicknesses of the CVD material.

Figure 1 shows AFM and PL images of a typical monolayer crystal with a small bilayer region at its center. The AFM images indicate that the deposited MoS₂ films are monolayer with a typical thickness of 0.9 nm. In addition, the enhancements of the PL signal emanating from the monolayer regions are indicative of the indirect-to-direct gap transition observed in MoS₂ as the layer count is reduced

from two or more layers to a single layer.¹ Single spectra recorded at 30 and 175 °C are shown in Figure 2, and extracted values of the temperature coefficient for the E_{2g}¹ and A_{1g} modes for both CVD grown monolayer and bulk (<100 nm thick) exfoliated MoS₂ are presented in Figure 3 and in Table I. An increased phonon coupling in the MoS₂ is observed at elevated temperatures, as shown in the increased intensity of the peaks for both monolayer (Figure 2) and bulk (not shown).

Any temperature-dependent changes in the calculated phonon density of states are due to the anharmonic terms in the lattice potential energy. In contrast to strictly harmonic

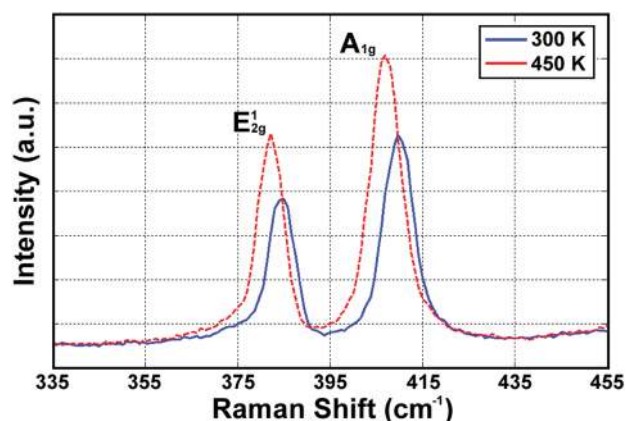


FIG. 2. Raman spectra of CVD monolayer MoS₂ taken at 30 °C and 175 °C plotted on the same scale showing the position of the E_{2g} in-plane and A_{1g} out-of-plane modes as well as an anomalous increase in intensity of the Raman signature.

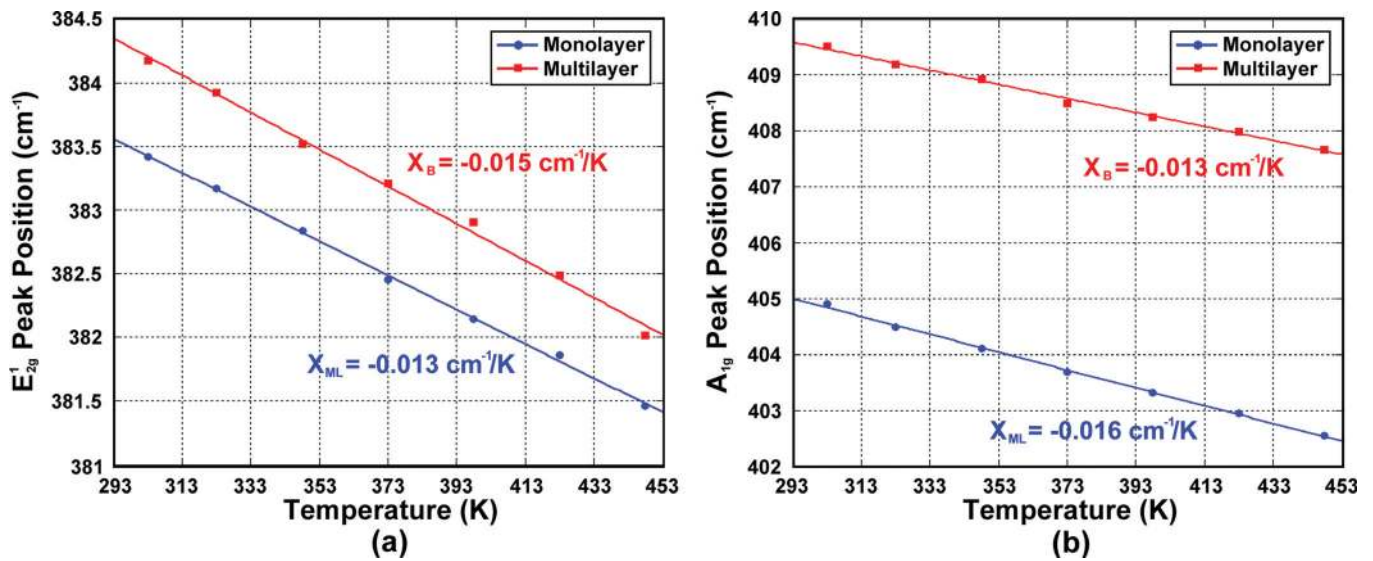


FIG. 3. Position of the E_{2g} (a) and A_{1g} (b) peaks as a function of temperature for CVD monolayer (red square) and exfoliated multilayer (blue circle) MoS_2 .

or quasi-harmonic calculations, anharmonic frequency shifts are the result of coupling between phonons having different momentum \mathbf{q} and band index j , as well as thermal expansion of the lattice. The calculated phonon density of states from molecular dynamics simulations at representative temperatures of 50 K and 300 K are shown in Figure 4.

At both temperatures, the Raman-active A_{1g} and E_{2g} peaks are well-defined, although slightly redshifted in frequency relative to estimates made in the harmonic approximation.¹³ It is clear that as the temperature is increased by several hundred Kelvin, both peaks shift toward lower frequencies, and that the frequency shift of the A_{1g} peak is more pronounced than that of the E_{2g} peak.

This temperature dependent shift of both peaks is due to the anharmonic contributions to the interatomic potential energy, mediated by phonon-phonon interactions. Intuitively, it makes sense that the out-of-plane A_{1g} mode shows a stronger temperature response in the monolayer, where there are no weak interlayer interactions restricting the vibrations away from the basal plane. While thermal expansion of the crystal is technically considered an anharmonic effect, it is a distinct physical phenomenon from the anharmonic coupling between phonons.²² Because the size of the supercell is held fixed during simulations at different temperatures, we expect thermal expansion to play a minimal role since the in-plane structure does not change appreciably.

We note that the A_{1g} mode has a stronger coupling to electrons than the E_{2g} mode, which could explain the larger frequency shift of the phonons. We can compare this to the

TABLE I. Comparison of the experimentally determined temperature coefficients (in units of cm^{-1}/K) for both bulk and monolayer MoS_2 as well as the frequency shifts calculated via molecular dynamics for the monolayer.

	X_B	X_{ML}	Δ_{ML}
A_{1g}	-0.013	-0.016	6 cm^{-1}
E_{2g}	-0.015	-0.013	3 cm^{-1}

case of superconducting MgB_2 , in which the anharmonic renormalization is greatest for the modes that couple most strongly to electrons.²³

In summary, we have used a combination of Raman spectroscopy and first-principles molecular dynamics simulations to study the temperature dependence of the Raman active peaks in monolayer MoS_2 . We have investigated the temperature dependence of the E_{2g} and A_{1g} peaks in the Raman spectra of monolayer MoS_2 grown by CVD on Si/SiO₂ substrates. Micro-Raman spectroscopy was carried out using the 532 nm laser excitation over the temperature range from 30 to 175 °C. The extracted values of the temperature coefficient of these modes are $X = -0.013 \text{ cm}^{-1}/^\circ\text{C}$ and $X = -0.016 \text{ cm}^{-1}/^\circ\text{C}$ for monolayer, and $X = -0.015 \text{ cm}^{-1}/^\circ\text{C}$ and $X = -0.013 \text{ cm}^{-1}/^\circ\text{C}$ for bulk, respectively. Simulation results agree qualitatively with experiment, predicting a larger temperature-dependent shift for the A_{1g} than for the E_{1g} mode.

We see that both the A_{1g} and E_{2g} peaks are redshifted with increasing temperature, and the magnitude of the A_{1g} temperature coefficient is larger than that of the E_{2g} mode. The temperature dependent shift of both peaks is attributed to anharmonic contributions in the interatomic potential

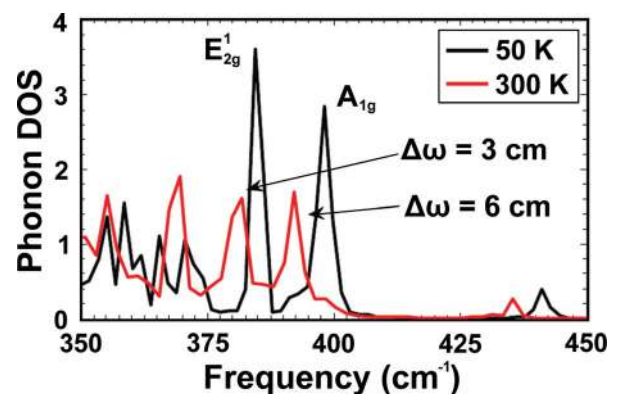


FIG. 4. The calculated phonon density of states for monolayer MoS_2 at temperatures of 50 K and 300 K.

energy due to phonon-phonon interactions. The larger anharmonic frequency shift of the A_{1g} mode is due to the stronger electron-phonon coupling relative to other Raman-active modes.

This study suggests that since the temperature coefficients of the Raman-active peaks in monolayer MoS₂ are distinct from those of the bulk, they can be used to positively identify single-layer samples in device applications. The temperature dependence of the Raman-active peaks will also affect the electron-phonon coupling, since the strength of the interaction is frequency dependent. This will in turn add a temperature dependence to the electron mobility in MoS₂-based field effect transistors. Future work will look at the temperature effects of few-layer MoS₂ as well as monolayers containing Mo defect sites.

This work used computational resources provided by the Computational Center for Nanotechnology Innovations (CCNI) at Rensselaer Polytechnic Institute. S.K.N. and N.A.L. acknowledge support by the Army Research Lab Multiscale Multidisciplinary Modeling of Electronic Materials (MSME) Collaborative Research Alliance (CRA), as well as experimental work supported by the Director's Strategic Initiative (DSI) program on interfaces and stacked 2D atomic layered materials. S.K.N. and N.A.L. would like to thank Interconnect Focus Center at Rensselaer supported by State of New York and an anonymous gift from Rensselaer for part of the support for this work. S.N. and J.L. acknowledge support from Welch Foundation grant C-1716 and NSF grant ECCS-1327093. Z.L. and P.M.A. acknowledge the support by U.S. Army Research Office MURI grant W911NF-11-1-0362, the U.S. Office of Naval Research MURI grant N000014-09-1-1066, and the FAME Center, one of six centers of STARnet, a Semiconductor

Research Corporation program sponsored by MARCO and DARPA.

- ¹K. Mak, C. Lee, J. Hone, J. Shan, and T. Heinz, *Phys. Rev. Lett.* **105**, 136805 (2010).
- ²A. Kuc, N. Zibouche, and T. Heine, *Phys. Rev. B* **83**, 245213 (2011).
- ³J. Ellis, M. Lucero, and G. Scuseria, *Appl. Phys. Lett.* **99**, 261908 (2011).
- ⁴A. Splendiani, L. Sun, Y. Zhang, T. Li, J. Kim, C. Chim, G. Galli, and F. Wang, *Nano Lett.* **10**, 1271 (2010).
- ⁵K. Kaasbjerg, K. Thygesen, and K. Jacobsen, *Phys. Rev. B* **85**, 115317 (2012).
- ⁶B. Radisavljevic, A. Radenovic, J. Brivio, V. Giacometti, and A. Kis, *Nat. Nanotechnol.* **6**, 147 (2011).
- ⁷B. Chakraborty, A. Bera, D. Muthu, S. Bhowmick, U. Waghmare, and A. Sood, *Phys. Rev. B* **85**, 161403 (2012).
- ⁸T. Livneh and E. Sterer, *Phys. Rev. B* **81**, 195209 (2010).
- ⁹C. Rice, R. J. Young, R. Zan, U. Bangert, D. Wolverson, T. Georgiou, R. Jalil, and K. S. Novoselov, *Phys. Rev. B* **87**, 081307 (2013).
- ¹⁰G. Kioseoglou, A. T. Hanbicki, M. Currie, A. L. Friedman, D. Gunlycke, and B. T. Jonker, *Appl. Phys. Lett.* **101**, 221907 (2012).
- ¹¹C. Lee, H. Yan, L. E. Brus, T. F. Heinz, J. Hone, and S. Ryu, *ACS Nano* **4**, 2695 (2010).
- ¹²P. Bertrand, *Phys. Rev. B* **44**, 5745 (1991).
- ¹³A. Molina-Sanchez and L. Wirtz, *Phys. Rev. B* **84**, 155413 (2011).
- ¹⁴C. Ataca, M. Topsakal, E. Akturk, and S. Ciraci, *J. Phys. Chem. C* **115**, 16354 (2011).
- ¹⁵T. Li, *Phys. Rev. B* **85**, 235407 (2012).
- ¹⁶These calculations used the code CPMD; Copyright IBM Corp 1990–2005, MPI für Festkörperforschung Stuttgart 1997–2001.
- ¹⁷S. Goedecker, M. Teter, and J. Hutter, *Phys. Rev. B* **54**, 1703 (1996).
- ¹⁸R. Car and M. Parrinello, *Phys. Rev. Lett.* **55**, 2471 (1985).
- ¹⁹S. Najmaei, Z. Liu, W. Zhou, X. Zou, G. Si, S. Lei, B. Yakobson, J. Idrobo, P. Ajayan, and J. Lou, *Nature Mater.* **12**, 754–759 (2013).
- ²⁰Y. Zhan, Z. Liu, S. Najmaei, P. Ajayan, and J. Lou, *Small* **8**, 966 (2012).
- ²¹S. Najmaei, Z. Liu, P. M. Ajayan, and J. Lou, *Appl. Phys. Lett.* **100**, 013106 (2012).
- ²²I. Calizo, A. A. Balandin, W. Bao, F. Miao, and C. N. Lau, *Nano Lett.* **7**, 2645 (2007).
- ²³M. Lazzeri, M. Calandra, and F. Mauri, *Phys. Rev. B* **68**, 220509 (2003).